

Synergistic effect of side-functionalization and aza-substitution on the charge transport and optical properties of perylene-based organic materials: A DFT study

Suryakanti Debata, Rudranarayan Khatua, Sridhar Sahu*

High Performance Computing lab, Department of Physics, Indian Institute of Technology
(Indian School of Mines) Dhanbad, India

E-mail: sridharsahu@iitism.ac.in

Section S1. EA and IP calculations

The adiabatic/vertical electron affinities and ionization potentials (AEAs/AIPs and VEAs/VIPs) of the studied compounds can be calculated from the potential energy surfaces (Figure S1) as follows.

$$\begin{aligned} \text{AEA} &= E - E_- \\ \text{AIP} &= E_+ - E \\ \text{VEA} &= E - E^* \\ \text{VIP} &= E^* - E \end{aligned}$$

+

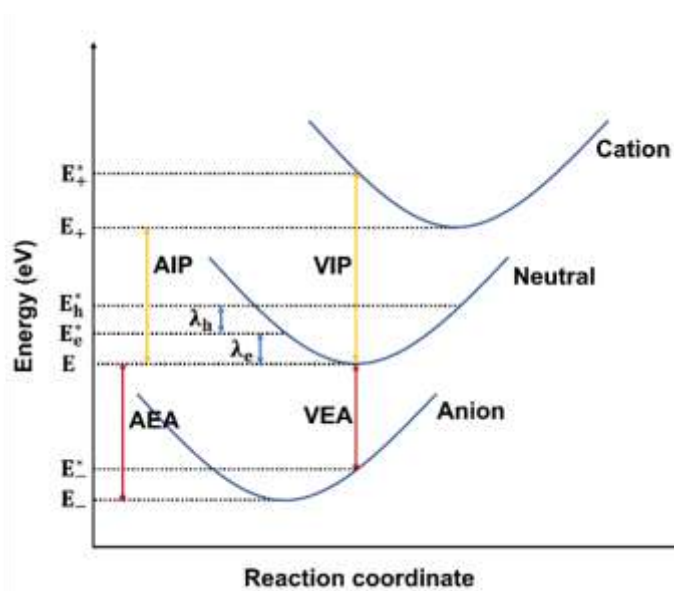


Figure S1. Schematic representation of potential energy surfaces of neutral and charged species of the organic semiconductors, used for calculating the internal hole/electron reorganization energies ($\lambda_{h/e}$) using four-point method, adiabatic/vertical electron affinities and ionization potentials (AEAs/AIPs and VEAs/VIPs).

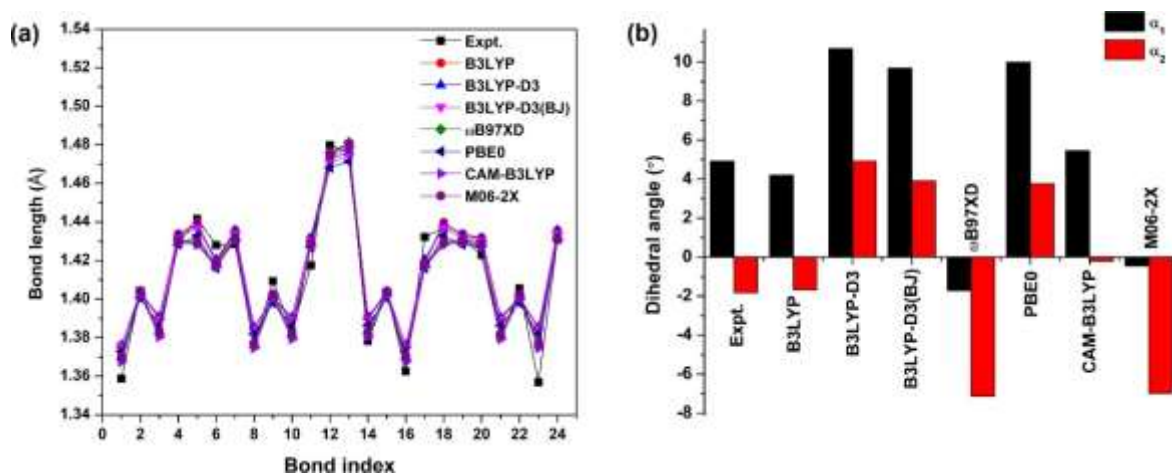


Figure S2. Deviation of geometrical parameters of **P1** at different levels of theory from the experimental values (a) bond lengths, and (b) dihedral angles.

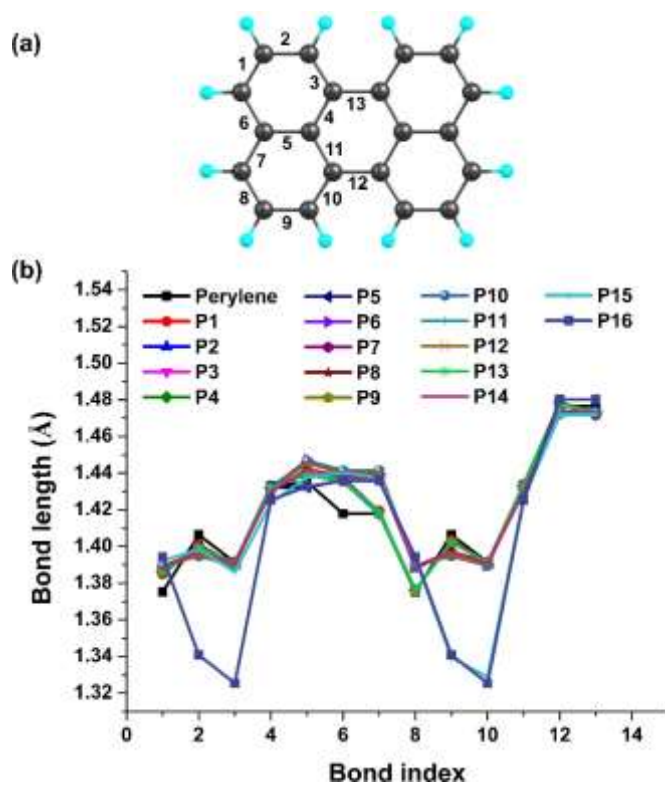


Figure S3. (a) optimized geometry of perylene using B3LYP/6-31G(d,p) method showing the selective bond labels, (b) bond-length deviations (in Å unit) at the selective sites of the studied compounds from the parent perylene structure upon side-substitution.

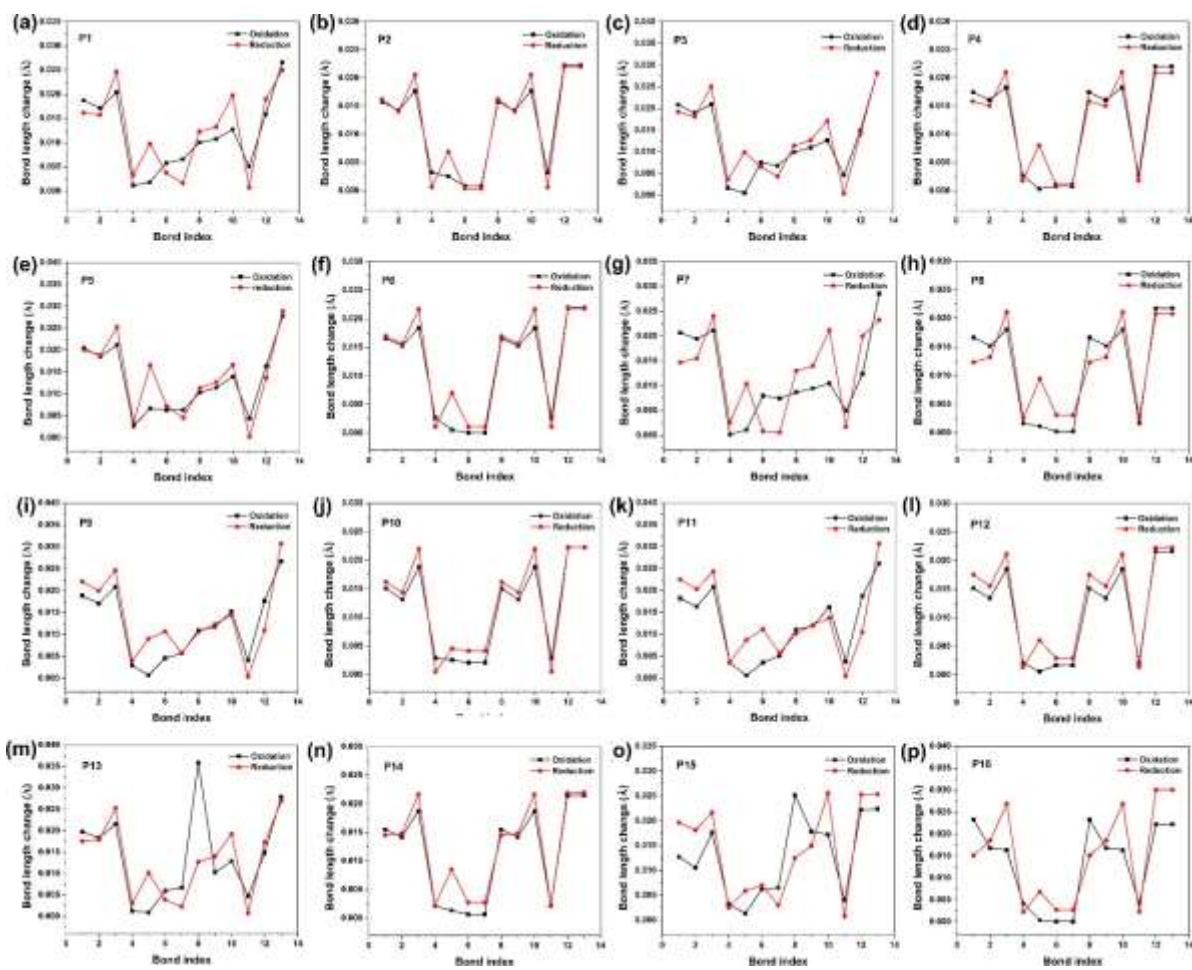


Figure S4. Bond-length changes (in Å unit) in the studied compounds during charge transfer.

Table S1. Unit-cell parameters of the crystals of perylene derivatives.

Compound	Crystal system	Space group	Packing motif	a	b (Å)	c	α	β (°)	γ
P1 [S1]	Orthorhombic	<i>Pbca</i>	Brick wall layer	12.51	35.54	16.82	90.0	90.0	90.0
P2 [S1]	Orthorhombic	<i>Pbca</i>	Herringbone	9.80	19.17	38.31	90.0	90.0	90.0
P3	Orthorhombic	<i>Pbca</i>	Herringbone	29.78	7.78	19.89	90.0	90.0	90.0
P4	Monoclinic	<i>Cc</i>	Brick wall layer	16.76	17.11	12.59	90.0	107.1	90.0
P5	Orthorhombic	<i>Pna2₁</i>	Herringbone	7.01	8.82	36.10	90.0	90.0	90.0
P6	Monoclinic	<i>P2₁/c</i>	Brick wall layer	16.17	21.16	9.86	90.0	101.1	90.0
P7	Orthorhombic	<i>P2₁2₁2₁</i>	Brick wall layer	35.05	6.95	9.05	90.0	90.0	90.0
P8	Orthorhombic	<i>Pbca</i>	Herringbone	29.61	10.98	18.98	90.0	90.0	90.0
P9	Orthorhombic	<i>Pbca</i>	Cofacial stacking	41.78	16.16	7.39	90.0	90.0	90.0
P10	Orthorhombic	<i>Pbca</i>	Herringbone	25.41	13.22	23.00	90.0	79.16	90.0
P11	Orthorhombic	<i>P2₁2₁2₁</i>	Cofacial stacking	4.28	34.81	16.31	90.0	90.0	90.0
P12	Orthorhombic	<i>Pbca</i>	Herringbone	24.54	13.17	22.55	90.0	90.0	90.0
P13	Orthorhombic	<i>Pbca</i>	Herringbone	10.01	7.67	61.70	90.0	90.0	90.0
P14	Orthorhombic	<i>Pbca</i>	Herringbone	17.76	31.22	12.42	90.0	90.0	90.0
P15	Orthorhombic	<i>P2₁2₁2₁</i>	Herringbone	13.01	11.74	22.81	90.0	90.0	90.0
P16	Orthorhombic	<i>P2₁2₁2₁</i>	Herringbone	22.98	11.68	12.86	90.0	90.0	90.0

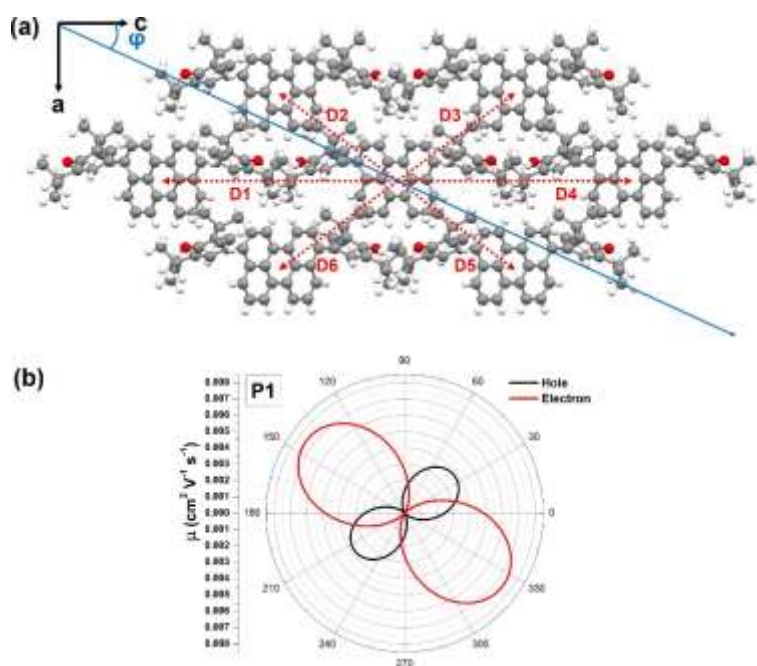


Figure S5. (a) Molecular crystal packing with illustration of different hopping pathways, and (b) anisotropic hole and electron mobilities of P1.

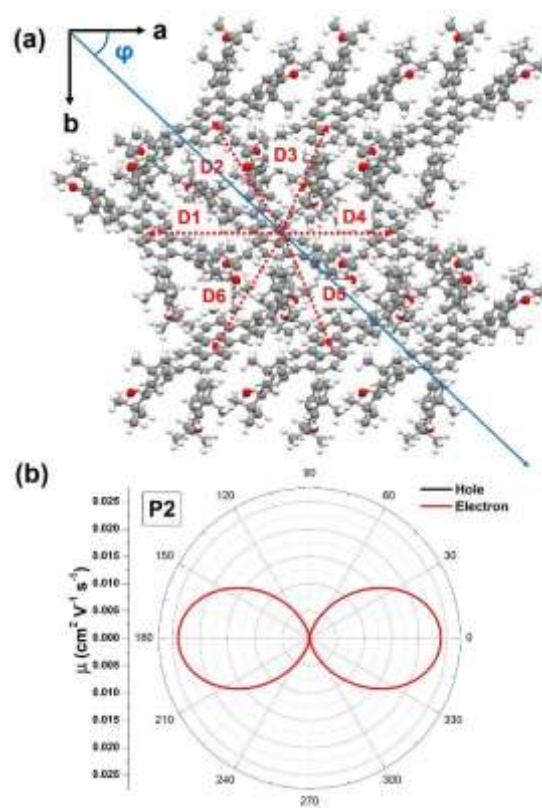


Figure S6. (a) Molecular crystal packing with illustration of different hopping pathways, and (b) anisotropic hole and electron mobilities of P2.

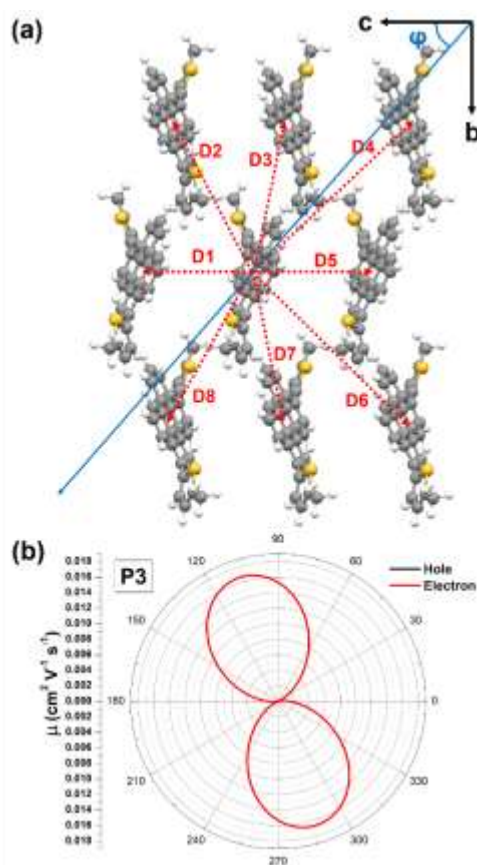


Figure S7. (a) Molecular crystal packing with illustration of different hopping pathways, and (b) anisotropic hole and electron mobilities of P3.

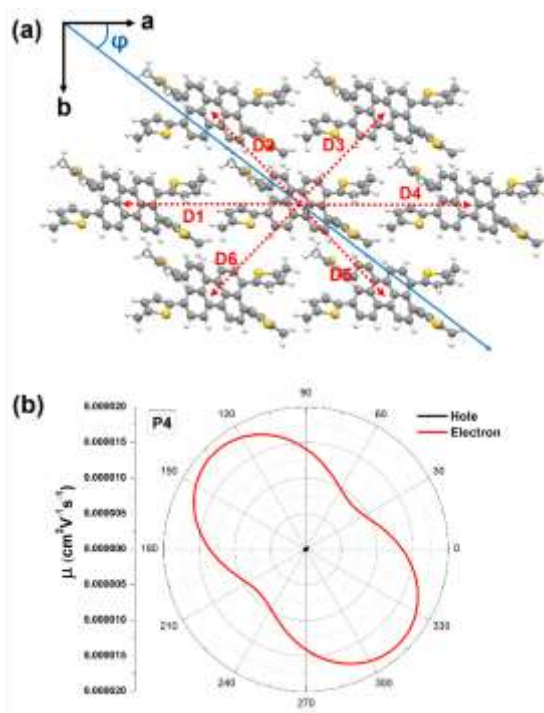


Figure S8. (a) Molecular crystal packing with illustration of different hopping pathways, and (b) anisotropic hole and electron mobilities of P4.

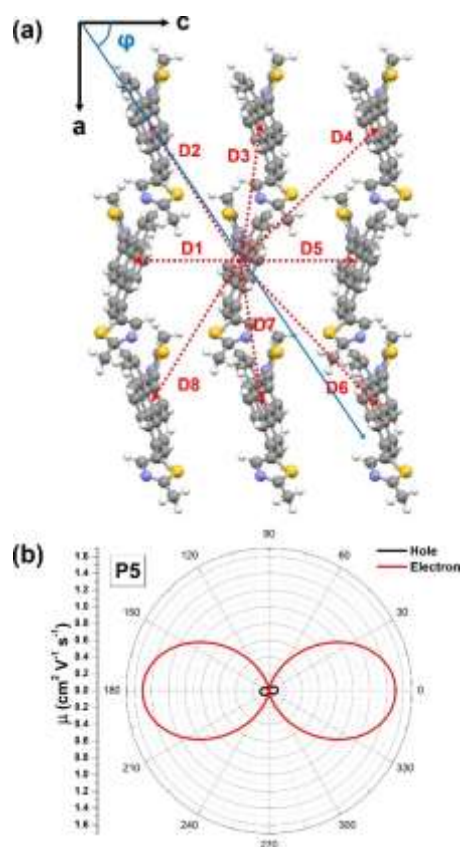


Figure S9. (a) Molecular crystal packing with illustration of different hopping pathways, and (b) anisotropic hole and electron mobilities of P5.

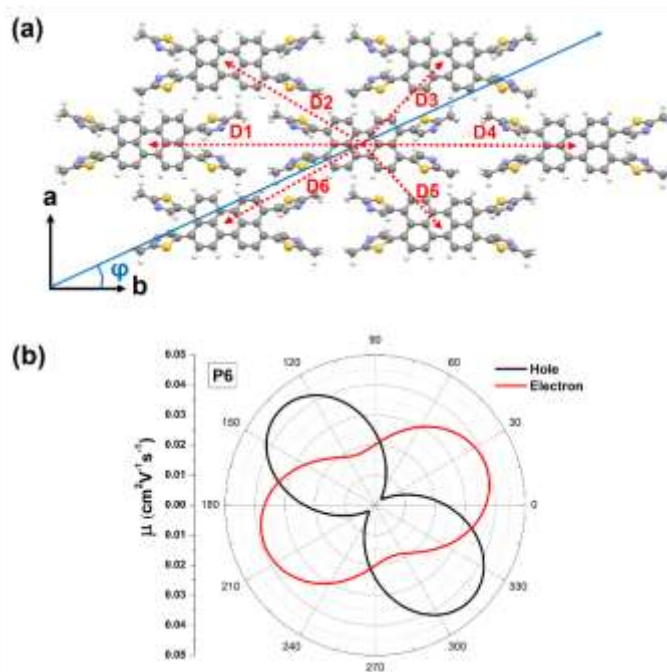


Figure S10. (a) Molecular crystal packing with illustration of different hopping pathways, and (b) anisotropic hole and electron mobilities of P6.

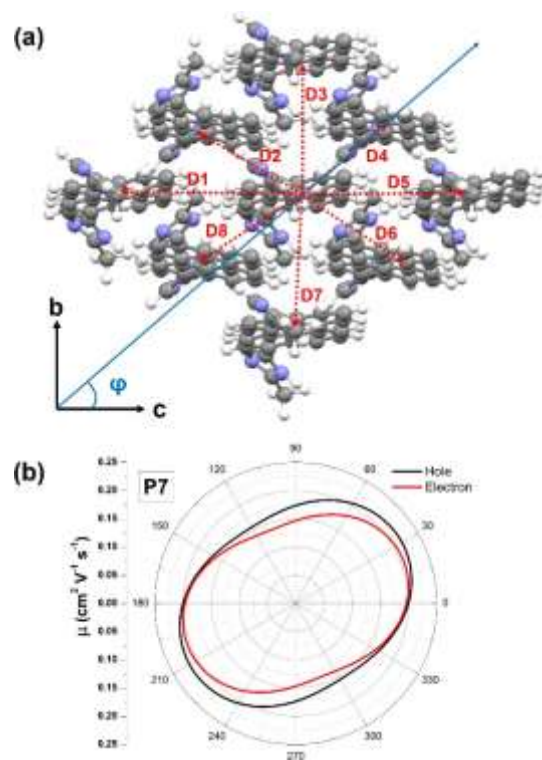


Figure S11. (a) Molecular crystal packing with illustration of different hopping pathways, and (b) anisotropic hole and electron mobilities of P7.

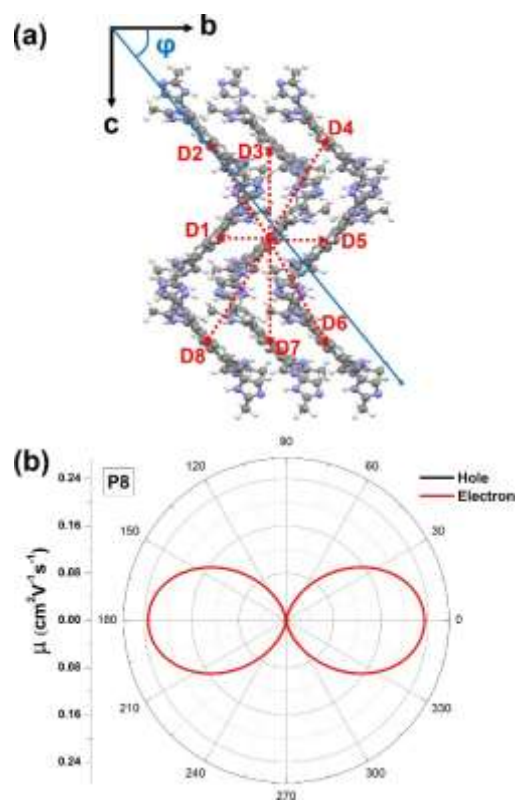


Figure S12. (a) Molecular crystal packing with illustration of different hopping pathways, and (b) anisotropic hole and electron mobilities of P8.

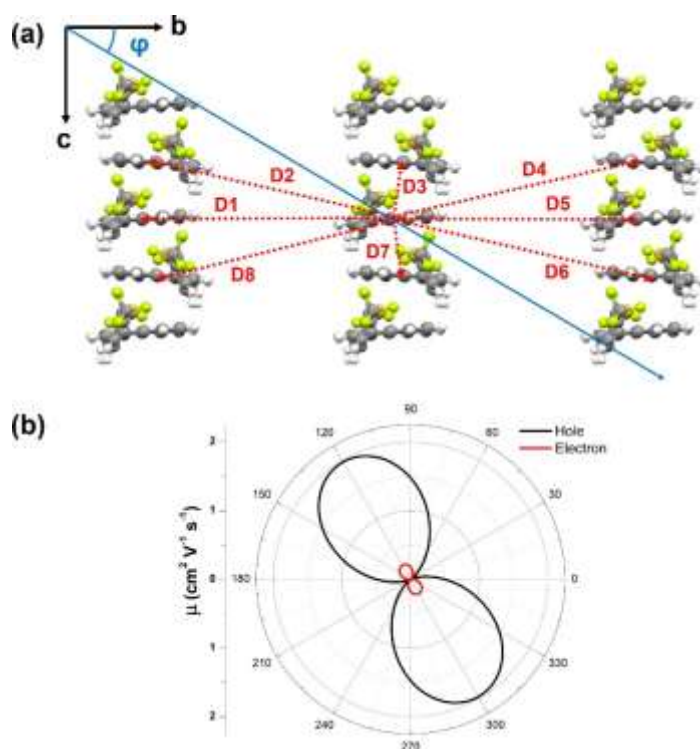


Figure S13. (a) Molecular crystal packing with illustration of different hopping pathways, and (b) anisotropic hole and electron mobilities of P9.

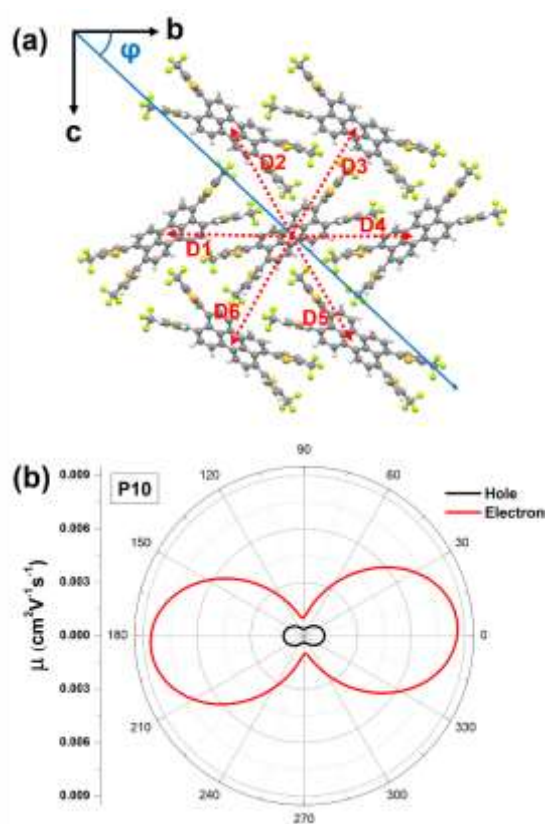


Figure S14. (a) Molecular crystal packing with illustration of different hopping pathways, and (b) anisotropic hole and electron mobilities of P10.

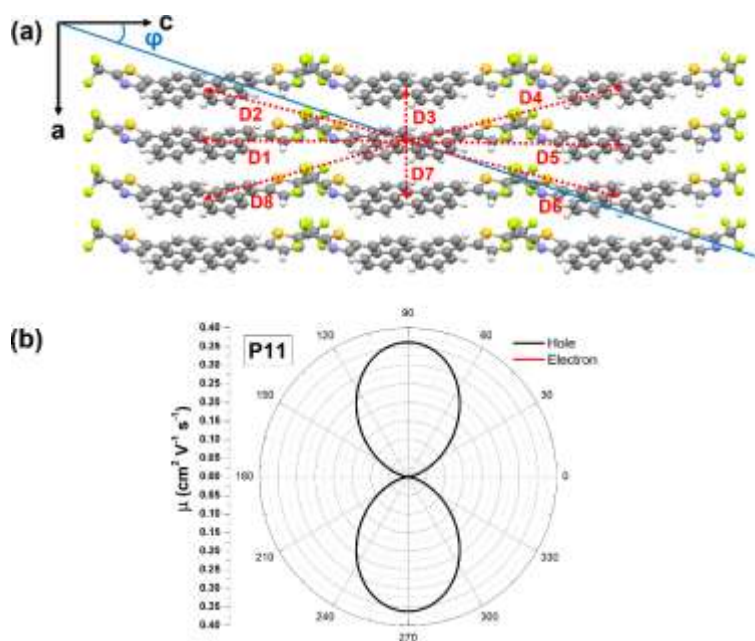


Figure S15. (a) Molecular crystal packing with illustration of different hopping pathways, and (b) anisotropic hole and electron mobilities of P11.

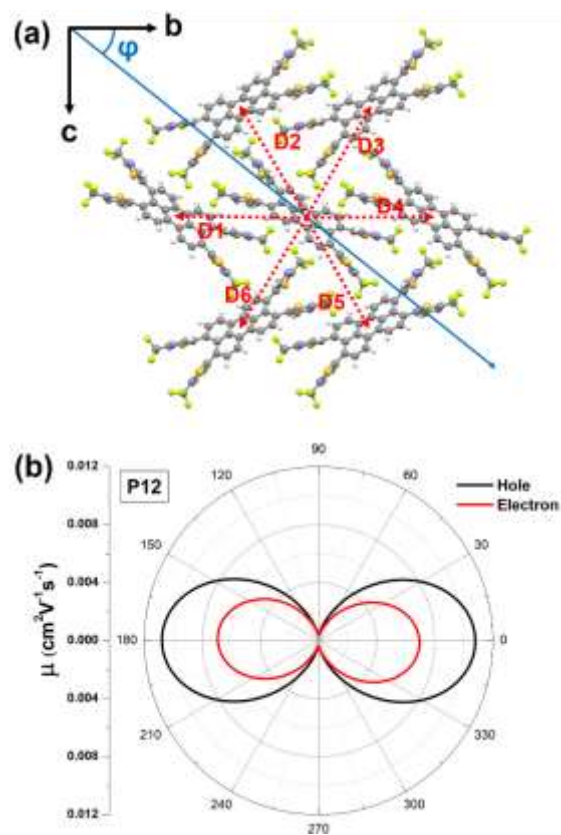


Figure S16. (a) Molecular crystal packing with illustration of different hopping pathways, and (b) anisotropic hole and electron mobilities of P12.

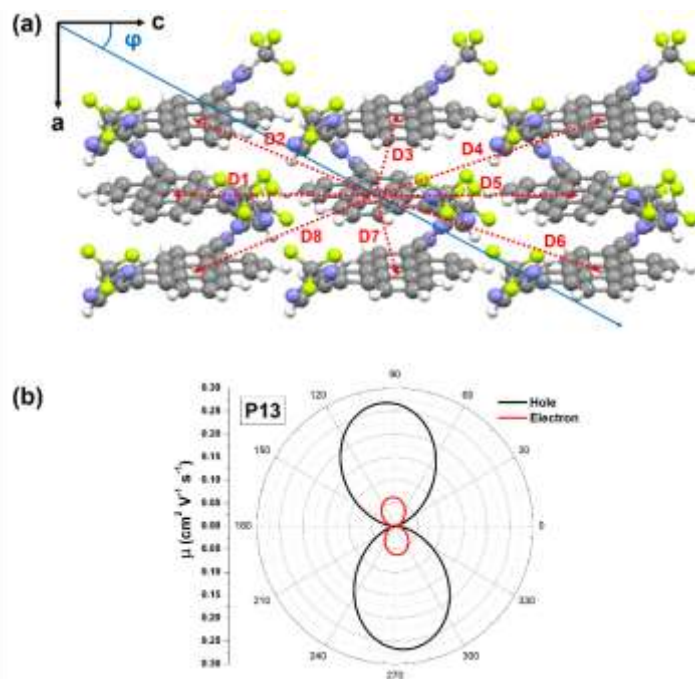


Figure S17. (a) Molecular crystal packing with illustration of different hopping pathways, and (b) anisotropic hole and electron mobilities of P13.

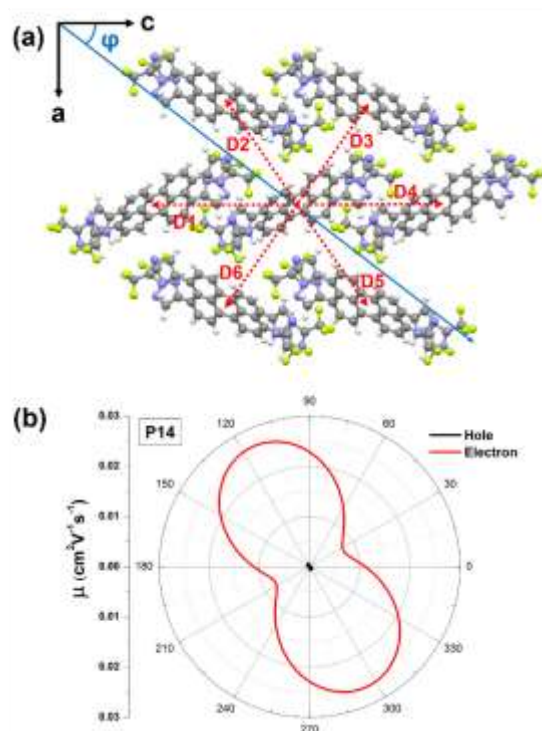


Figure S18. (a) Molecular crystal packing with illustration of different hopping pathways, and (b) anisotropic hole and electron mobilities of P14.

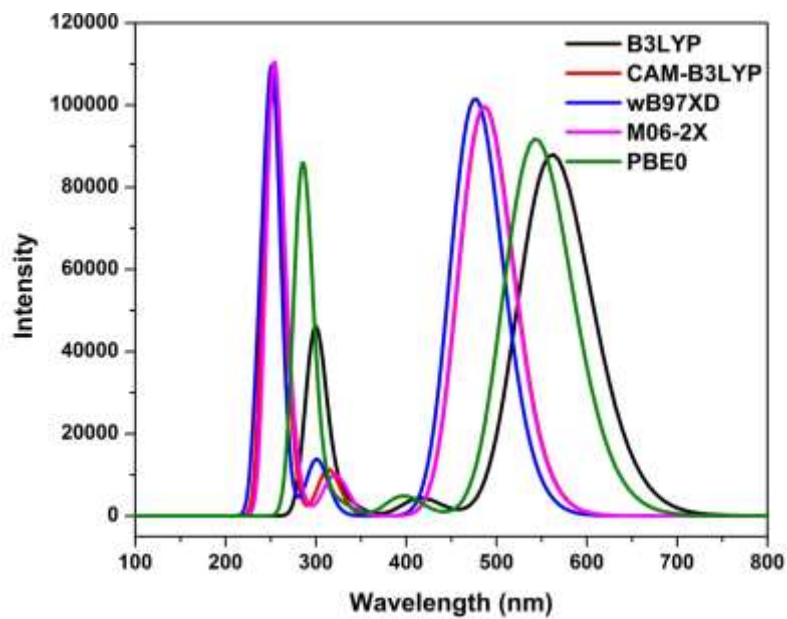


Figure S19. Benchmarking of TD-DFT method by comparing the absorption spectra of **P2** obtained with different exchange-correlation functionals.

Reference

- S1. Y. Hirao, T. Okuda, Y. Hamamoto, T. Kubo, Formation of perylenes by oxidative dimerization of naphthalenes bearing radical sources, *ChemPlusChem* 2019, 84, 1–10.